Hindawi Publishing Corporation
EURASIP Journal on Wireless Communications and Networking
Volume 2009, Article ID 263695, 11 pages
doi:10.1155/2009/263695

Research Article

Residue Number System Arithmetic Assisted Coded Frequency-Hopped OFDMA

Dalin Zhu and Balasubramaniam Natarajan

Department of Electrical & Computer Engineering, Kansas State University, 2061 Rathbone Hall, Manhattan, KS 66506, USA

Correspondence should be addressed to Dalin Zhu, dalinz@ksu.edu

Received 31 July 2008; Revised 17 December 2008; Accepted 23 February 2009

Recommended by Lingyang Song

We propose an RNS arithmetic-based FH pattern design approach that is well suited and easy to implement for practical OFDMA systems. The proposed FH scheme guarantees orthogonality among intracell users while randomizing the intercell interferences and providing frequency diversity gains. We present detailed construction procedures and performance analysis for both independent and cluster hopping scenarios. Using simulation results, we demonstrate the gains due to frequency diversity and intercell interference diversity on the system bit error rate (BER) performance. Furthermore, the BER performance gain is consistent across all cells unlike other FH pattern design schemes such as the Latin squares (LSs-)-based FH pattern design where wide performance variations are observed across cells.

1. Introduction

Orthogonal frequency division multiplexing (OFDM) has been widely accepted as an enabling technology for next generation wireless communication systems. In OFDM, high-rate data streams can be broken down into a number of parallel lower-rate streams, thereby avoiding the need for complex equalization. OFDM also forms the foundation for a multiple access scheme termed as orthogonal frequency division multiple access (OFDMA). In OFDMA, each user is assigned a fraction of available subcarriers based upon his/her demand for bandwidth. The advantages of OFDMA include (1) the flexibility in subcarriers' allocation; (2) the absence of multiuser interference due to subcarriers' orthogonality; (3) the simplicity of the receiver design [1].

In order to enhance system throughput and spectral efficiency, frequency hopping (FH) is generally used in OFDMA cellular systems. It is desirable for FH patterns to satisfy the following conditions [2]: (i) minimize intracell interference; (ii) average intercell interference; (iii) avoid ambiguity while identifying users; (iv) exploit frequency diversity by forcing hops to span a large bandwidth. The first aspect is relatively easy to achieve by using orthogonal hopping patterns within a cell. To average intercell interferences, hopping patterns are constructed in a way that two users in different cells interfere with each other only during a small fraction of all hops. The third condition requires base stations to have the capability of distinguishing different users efficiently according to their unique FH signatures. Finally, the last requirement not only ensures the security of the transmission, but also mitigates the effect of fading by exploiting frequency diversity.

Frequency hopping pattern design has received considerable attention in both commercial and military communication systems. There has been extensive work on designing FH-OFDMA systems [3–10]. In [3], concepts of fast frequency hopping along with OFDM are illustrated. In [4], authors show that the expected number of collisions per symbol under both independent and cluster hopping does not depend on the hopping strategy. In their later work [5], it is shown that the number of collisions can be further reduced by using space-frequency coding in multiple-antenna systems. Orthogonal Latin squares (LSs) are presented as FH patterns in TCM/BICM coded OFDMA in [6]. In LS-aided FH-OFDMA systems, it is seen that there is a wide variability in the performance of users in different cells. Therefore, it is not an effective scheme if one considers fairness to be important. Welch-Costas array is introduced in [7] and evaluated in [8] for coded

FH-OFDMA. Here, although users across cells experience significant performance improvements, users within a cell may not occupy all of the available bandwidth to exploit full frequency diversity. Other aspects focusing on preventing hostile jamming and pilot-assisted channel estimation in FH-OFDMA are explored in [9, 10], respectively.

In this paper, we propose a novel frequency hopping pattern design strategy based on RNS arithmetic for practical OFDMA cellular systems. We show that the resulting patterns are orthogonal within a cell and intersect only once across cells in a frequency hopping cycle. RNS arithmetic has found applications in many areas. However, its use in designing frequency hopping patterns is rarely considered [11, 12]. In [11], the design procedure can be visualized as a "top-down" approach where a given bandwidth is divided into multiple candidate subbands based on a predetermined moduli set. As a result, if the moduli set changes, the bandwidth of subcarriers varies. In this work, the division of bandwidth into candidate subcarriers is assumed to be given or determined in advance. Therefore, we can consider our proposed approach as a "bottom-up" method driven by grouping and indexing the subcarriers according to the RNS arithmetic. For practical OFDMA cellular systems, the proposed "bottom-up" approach is more feasible. For example, in downlink OFDMA cellular systems, a fixed number of subcarriers (e.g., 1024) with identical subcarrier bandwidth within each cell is usually assumed. Furthermore, for reducing intercell interference, [11] suggests the use of different moduli sets for adjacent cells. This approach results in adjacent cells employing different numbers of subcarriers with different bandwidths across cells. Once again, this is a stringent requirement that may not be feasible in practice. In this work, we invoke the use of the so-called two-stage and multistage selection algorithms to construct RNS-FH patterns such that (1) different users can use the spectral resources simultaneously within each cell and (2) the same number of subcarriers can be employed from cell to cell. Additionally, the proposed FH sequences force the intracell interferences to zero and average out the intercell interferences. The performance of the proposed FH pattern incorporating with both independent and cluster hopping schemes is characterized. Simulation results show that RNS-FH OFDMA has significantly better BER performance relative to traditional OFDMA scheme without FH. Another aspect that makes RNS-FH pattern design outperforms other existing FH techniques is that user hopping patterns span a larger bandwidth. Therefore, the channel fades associated with consecutive hops become independent. Moreover, with the use of FEC codes over multiple hops, the system can correct errors due to subcarriers that experience deep fades or subcarriers that are severely interfered by others.

The rest of the paper is organized as follows. In Section 2, system model along with signal transmission scheme, access strategies, and interference models is introduced. In Section 3, detailed RNS-FH pattern design procedures along with comparisons with the existing technique are presented. Simulation results with performance analysis are given in Section 4. Finally, we conclude this paper in Section 5.

2. System Model

In this section, we first describe the signal transmission scheme for each individual user in an OFDMA system. Then, we introduce the access model and interference model under both independent and cluster hopping schemes.

2.1. Signal Transmission Scheme. The block diagram of FEC coded FH-OFDMA system is shown in Figure 1. Here, data bits of every user are first channel coded and then mapped to complex constellation points. We assume that there are M users in the system, utilizing a total of N OFDM subcarriers. Each user is assigned a specific set of subcarriers out of the total available subcarriers according to his/her data rates. Let N_i be the number of subcarriers allocated to user i. Then, user i transmits the information symbols $\mathbf{x}^i = (x_1^i, x_2^i, \ldots, x_{N_i}^i)^T$ ($(\cdot)^T$ represents the transpose operation) on the assigned N_i subcarriers. Therefore, the baseband transmitted signal of user i can be expressed as

$$s^i(t) = \sum_{k=1}^{N_i} x_k^i e^{j2\pi(k/T)t}, \quad 0 \le t < T, \tag{1}$$

where $s^i(t)$ represents the time-domain signal, and T denotes one OFDM symbol duration. Since this is an OFDMA system, it is important to remember that every user is assigned a different set of subcarriers for transmission, and this allocation is dynamic in the case of frequency hopping OFDMA. That is, in the IFFT module, the frequency assignment follows a predetermined FH pattern. Moreover, each user transmits zeros on subcarriers which are not assigned to him/her.

For convenience, we note C_i as the subcarrier that is assigned to user i. Hence, $N \times 1$ information symbols vector of user i can be written as

$$\mathbf{x}^i(k) = \begin{cases} 0, & k \notin C_i, \\ x_k^i, & k \in C_i. \end{cases} \tag{2}$$

The discrete form of the transmitted signal $s^i(t)$ is then given as,

$$\mathbf{s}^i = \mathbf{F}\mathbf{x}^i, \tag{3}$$

where $\mathbf{F}$ is the IFFT matrix defined as

$$\mathbf{F} = \frac{1}{\sqrt{N}} \begin{pmatrix} W_N^{00} & \cdots & W_N^{0(N-1)} \\ \vdots & \ddots & \vdots \\ W_N^{(N-1)0} & \cdots & W_N^{(N-1)(N-1)} \end{pmatrix}, \tag{4}$$

where $W_N^{pq} = e^{j2\pi pq/N}$.

Let $\mathbf{h}^i = [h^i(0), h^i(1), \ldots, h^i(N-1)]$ denote the channel impulse response vector, then its Fourier transform is

$$\mathbf{H}^i = \mathbf{F}^H \mathbf{h}^i, \tag{5}$$

where $(\cdot)^H$ represents the Hermitian transpose. In general, each channel impulse response is a function of time and

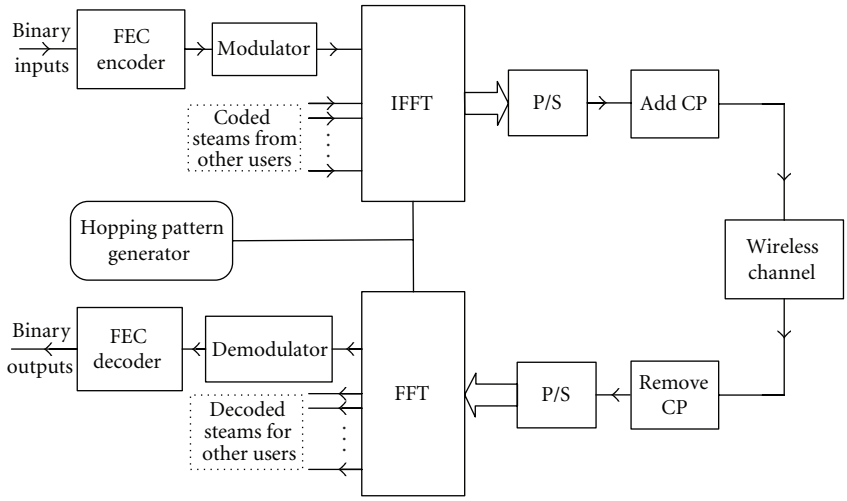

Figure 1: The block diagram of coded FH-OFDMA system.

access delay which can be modeled as a tapped delay line, that is,

$$h^i(\tau,t)=\sum_{l=1}^{L}h_l^i(t)\delta(\tau,\tau_l), \tag{6}$$

where L is the number of multipaths and τ_l is the time delay of the lth path. The tap coefficients are independent, zero mean, circularly symmetric complex Gaussian random processes at each instant t, that is, $h_l^i(t)\sim CN(0,\sigma_l^2)$ with the total power normalized to unity, that is, $\sum_{l=1}^{L}\sigma_l^2=1$. In this work, we use Jakes' model to describe the time/frequency variation of each channel coefficient. Therefore, the spaced frequency (Δf) spaced time (Δt) correlation function of the channel frequency response can be expressed as [13]

$$r_H(\Delta f,\Delta t)=\sum_{l=1}^{L}\sigma_l^2J_o(2\pi f_D\Delta t)e^{-j2\pi\Delta f\tau_k}, \tag{7}$$

where f_D is the Doppler frequency.

At the receiver end, after FFT, the received signal corresponding to user i on subcarrier k is

$$\mathbf{r}^i(k)=\mathbf{H}^i(k)\mathbf{x}^i(k). \tag{8}$$

Then, the overall received signal which is a superposition of the signals transmitted from all M users is

$$\begin{aligned}\mathbf{r}(k)&=\sum_{i=1}^{M}\mathbf{r}^i(k)+\mathbf{n}(k)\\&=\sum_{i=1}^{M}\mathbf{H}^i(k)\mathbf{x}^i(k)+\mathbf{n}(k),\end{aligned} \tag{9}$$

where $\mathbf{n}(k)$ is the Fourier transform of the noise vector.

2.2. Access Model. In this part, clustered and independent FH-OFDMA are introduced, and closed form expressions of the expected number of collisions per symbol under both of these two hopping strategies are presented.

2.2.1. Clustered FH-OFDMA. In cluster hopping, each user selects a set of continuous subcarriers, termed cluster, to transmit the information symbols. Specifically, the hopping takes place among clusters of subcarriers based on predetermined FH patterns. Therefore, collisions occur among clusters first, and then across all OFDM subcarriers within that cluster. The expected number of symbol losses per cluster collision corresponds to [4]

$$E_c=N_cP_{\text{int}}, \tag{10}$$

where N_c is the number of subcarriers per cluster and P_{int} represents the probability that at least one interfering user collides with the desired user. For cluster hopping, we have N/N_c hopping clusters. Therefore, the collision probability between the desired user and the interfering user in one cluster is $1/(N/N_c)$. Hence, the probability that at least one of the $M-1$ users collides with the desired user can be expressed as

$$P_{\text{int}}=1-\left(1-\frac{1}{N/N_c}\right)^{M-1}. \tag{11}$$

For convenience, throughout the rest of this paper, we assume that each user employs the same number of subcarriers (N_c) per cluster.

2.2.2. Independent FH-OFDMA. In independent hopping, subcarriers occupied by a user are selected independently from all available subcarriers. In other words, N_c subcarriers in one cluster are not continuous anymore, and they are chosen in a pseudorandom fashion across the frequency spectrum. With independent hopping, the expected number of symbols lost per symbol collision is given by [4]

$$E_{\tilde{c}}=\sum_{x=1}^{N_c}xp_{N_c}(x), \tag{12}$$

where $p_{N_c}(x)$ is the probability that x subcarriers out of N_c subcarriers occupied by each user experience collisions due to interfering users.

Theorem 1. *For independent FH-OFDMA scheme described above, $p_{N_c}(x)$ corresponds to*

$$p_{N_c}(x) = \binom{N_c}{x}\left[1-\left(\frac{N-2N_c+x}{N-N_c+x}\right)^{M-1}\right]^{x} \times \left(\prod_{y=0}^{N_c-1}\frac{N-N_c+x-y}{N-y}\right)^{M-1}. \tag{13}$$

Proof. $p_{N_c}(x)$ is the probability that x subcarriers of the desired user collide with the subcarriers of interfering user given that each user occupies a total of N_c subcarriers. It is evident that the number of possible combinations of x subcarriers that experience collisions is $\binom{N_c}{x}$. Define $q_{N_c}(a)$ as the probability that a symbols are collision-free given that each user occupies N_c subcarriers. Furthermore, define $p_{N_c}(b \mid c)$ as the conditional probability that b symbols collide given that c symbols are collision-free. Therefore, we can write $p_{N_c}(x)$ as

$$p_{N_c}(x) = \binom{N_c}{x} q_{N_c}(N_c-x)\, p_{N_c}(x \mid N_c-x). \tag{14}$$

Here, $q_{N_c}(N_c-x)$ corresponds to

$$q_{N_c}(N_c-x) = \left(\prod_{k=0}^{N_c-1}\frac{N-(N_c-x)-k}{N-k}\right)^{M-1}. \tag{15}$$

Equation (15) denotes the probability that the desired user's remaining $N_c - x$ subcarriers are collision-free while none of the other $M-1$ users within the same cell occupies these subcarriers. $p_{N_c}(x \mid N_c-x)$ is expressed as [4]

$$p_{N_c}(x \mid N_c-x) = \left[1-\left(\frac{N-2N_c+x}{N-N_c+x}\right)^{M-1}\right]^{x}. \tag{16}$$

Equation (16) represents the conditional probability that each of the x subcarriers of the desired user collides given that the other $N_c - x$ subcarriers are collision-free. By substituting (15) and (16) into (14), we obtain the result in (13). □

2.3. Interference Model. In this paper, we model intercell interferences as additive complex Gaussian-distributed distortions. This model is accurate when interferences from adjacent cells are perfectly randomized with respect to the cell of interest. Models specific to clustered and independent FH-OFDMA are presented in the following.

2.3.1. Clustered FH-OFDMA. In clustered FH-OFDMA, if interference occurs on any symbol on one subcarrier in the cluster, all other symbols in the same cluster will also experience interferences from adjacent cells. Hence, the interference for the ith user can be modeled as [6]

$$\mathbf{r}^i = \mathbf{H}^i\mathbf{x}^i + \mathbf{n}^i + \mathbf{e}^i, \tag{17}$$

where $\mathbf{r}^i$ is an $N_c \times 1$ vector, representing the received signal of user i; $\mathbf{x}^i$ is the $N_c \times 1$ transmitted signal vector; $\mathbf{H}^i$ is an $N_c \times N_c$ matrix that contains the frequency domain representations of channel impulse response; $\mathbf{n}^i$ is an $N_c \times 1$ vector whose components are complex Gaussian random variables with zero mean and variance σ^2. Here, the $N_c \times 1$ vector $\mathbf{e}^i$ is the interference vector that captures the interference from all adjacent cells. The components of $\mathbf{e}^i$ are i.i.d complex Gaussian random variables independent of $\mathbf{x}^i$, $\mathbf{H}^i$ and $\mathbf{n}^i$ with mean zero, variances $(\widetilde{\sigma}_1^2,\ldots,\widetilde{\sigma}_{N_c}^2)^T$. The variances correspond to

$$\widetilde{\sigma}_j^2 = \frac{\rho E_s}{\mathrm{SIR}_s}, \quad j = 1,2,\ldots,N_c, \tag{18}$$

where SIR_s denotes the symbol signal-to-interference ratio and $\rho \in \{1,0\}$ characterizes the presence/absence of a collision between users in different cells. That is, if there is a collision, ρ equals to one; if there is no collision, ρ is set to zero. Furthermore, ρ can be modeled as Bernoulli's random variable with probability of collision equals to p (i.e., $P(\rho=1)=p$ and $P(\rho=0)=1-p$), which can be expressed as

$$p = 1-\left(1-\frac{1}{N/N_c}\right)^{M-1}, \tag{19}$$

where M is the number of active users. If the system is fully loaded, then $M = N/N_c$. If there is a collision, that is, $\rho = 1$, then all subcarriers in the cluster will be affected by the intercell interference.

2.3.2. Independent FH-OFDMA. In independent hopping, since subcarriers are selected independently of all other subcarriers according to predetermined FH patterns, collisions occur independently. Hence, for the kth subcarrier of the ith user,

$$\mathbf{r}^i(k) = \mathbf{H}^i(k)\mathbf{x}^i(k) + \mathbf{n}^i(k) + \mathbf{e}^i(k). \tag{20}$$

Here, the interference power $\widetilde{\sigma}^2$ of the i.i.d complex Gaussian random variable $\mathbf{e}^i(k)$ corresponds to

$$\widetilde{\sigma}^2 = \frac{\rho E_s}{\mathrm{SIR}_s}, \tag{21}$$

where $\rho = 1,0$ with probabilities p and $1-p$, respectively. The collision probability p is given by

$$p = 1-\left(1-\frac{1}{N}\right)^{MN_c-1}. \tag{22}$$

For a fully loaded system with independent hopping, M is identical to N, N_c becomes to one.

3. RNS-FH Pattern Design

RNS is defined by the choice of v number of positive integers m_i $(i = 1,2,\ldots,v)$, referred to as moduli [14]. If all the moduli are pairwise relative primes to each other, any integer N_k which falls in the range of $[0, M_r)$ can be uniquely and unambiguously represented by the residue sequence

$(r_{k,1}, r_{k,2}, \ldots, r_{k,v})$, where $M_r = \prod_{i=1}^{v} m_i$ and $r_{k,i} = N_k$ *textmod* $\{m_i\}$ for $i = 1, 2, \ldots, v$. Here, N_k is used to describe the kth user FH address. To recover N_k, or to distinguish users at the base station, Chinese remainder theorem (CRT) is generally used which is well known for its capability of solving a set of linear congruences, simultaneously. According to CRT, it can be shown that the numerical value of N_k can be computed as [15]

$$N_k = \sum_{i=1}^{v} r_{k,i} a_i M_i \bmod M_r, \tag{23}$$

where $M_i = M_r/m_i$ and $a_i = M_i^{-1} \bmod \{m_i\}$ for $i = 1, 2, \ldots, v$.

Theorem 2. *The residue sequences obtained using the RNS arithmetic as described above are orthogonal.*

Proof. In order to prove that the residue sequences are orthogonal, we need to show that every N_k in the range of $[0, M_r)$ has a unique residue set that is different from residue sets generated by other integers within the same range. We will prove this by contradiction as follows.

Assuming that N_1 and N_2 are different integers which are in the same range of $[0, M_r)$ with the same residue set. That is,

$$N_1 \bmod \{m_i\} = N_2 \bmod \{m_i\}, \quad i = 1, 2, \ldots, v. \tag{24}$$

Therefore, we have

$$(N_1 - N_2) \bmod \{m_i\} = 0. \tag{25}$$

Thus, we can conclude from (25) that $N_1 - N_2$ is actually the least common multiple (LCM) of m_i. Furthermore, if m_i are pairwise relative primes to each other, their LCM is $M_r = \prod_{i=1}^{v} m_i$ and it must be that $N_1 - N_2$ is a multiple of M_r. However, this statement does not hold since $N_1 < M_r$ and $N_2 < M_r$. Therefore, by contradiction, N_1 and N_2 should not have the same residue set. In general, the residue set $(r_{k,1}, r_{k,2}, \ldots, r_{k,v})$ generated by N_k is unique and can be used to represent the integer N_k if $N_k < M_r$. □

Following the RNS arithmetic presented above, we propose to design FH patterns that satisfy all the requirements described in Section 1 while avoiding the limitations in [11]. Detailed procedures of constructing RNS-FH patterns are given in the following subsections. The first part describes the two-stage algorithm, while the second part introduces the multistage algorithm which can be considered as generalization of the two-stage algorithm. At the end of this section, we compare our proposed RNS-FH pattern design strategy with the method presented in [11].

3.1. Two-Stage Algorithm. In this part, the detailed procedures of constructing RNS-FH patterns via the so-called two-stage algorithm is introduced. We present the algorithm for a cluster hopping OFDMA system. It is straightforward to extend the algorithm to the independent hopping scenario. The steps involved in the two-stage selection algorithm are given as follows.

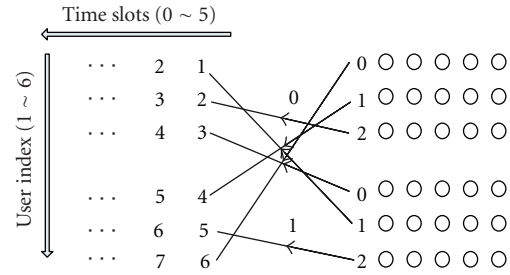

Figure 2: One example of RNS-assisted two-stage hopping strategy.

(1) Divide the total available subcarriers N into M_c clusters with each cluster containing N_c number of contiguous subcarriers.

(2) If M_c can be written as a product of two pairwise relative primes, for example, $M_c = a_1 \cdot b_1$, we can first group M_c clusters into a_1 groups with b_1 clusters in each group. Then, we index the groups from 0 to $a_1 - 1$.

(3) Index the clusters in each group from 0 to $b_1 - 1$.

(4) At the 0th time slot, assign integer N_k to user k as its FH address according to its access order to the system, where $0 < N_k \leq M_c$.

(5) If $N_k \bmod \{a_1, b_1\} = \{\hat{a}_1, \hat{b}_1\}$, then user k selects the $\hat{b}_1$th cluster out of the $\hat{a}_1$th group for transmission.

(6) At the t_sth time slot, assign integer $N_k + t_s$ to user k as its current FH address and repeat step 5.

(7) Repeat steps 4–6 until one mutually orthogonal FH pattern is obtained.

(8) If M_c can be expressed as products of other combinations of two pairwise relative primes, for example, $M_c = a_2 \cdot b_2 = \cdots = a_w \cdot b_w$, then w different orthogonal FH patterns can be obtained by repeating steps 2–7, w times.

An example is given in Figure 2 to illustrate the two-stage RNS-assisted frequency hopping strategy. Here, 6 users access the system ($M = 6$); the total number of subcarriers is 30 ($N = 30$) and they are divided into 6 clusters ($M_c = 6$) with each cluster containing 5 contiguous subcarriers ($N_c = 5$). At the 0th time slot, the FH address assigned to the 5th user is 5 according to his/her access order to the system. Therefore, $5 \bmod \{2, 3\} = \{1, 2\}$. User 5 will choose the 2nd cluster of subcarriers out of the 1st group of clusters to transmit. At the 1st time slot, the FH address assigned to this user becomes $5 + 1 = 6$. Obviously, $6 \bmod \{2, 3\} = \{0, 0\}$, then he/she will select the 0th cluster of subcarriers out of the 0th group of clusters for transmission at this time. This process continues until one FH sequence of length M_c is constructed.

3.2. Multistage Algorithm. The multistage algorithm is an extension of the two-stage algorithm. Introducing the multistage algorithm cannot only enhance the flexibility of the

pattern design, but also strengthen the robustness of the entire FH scheme. We describe the multistage algorithm assuming an independent hopping scheme with each user employing the same number of subcarriers, that is, $N_i = N_c$ for $i = 1, 2, \ldots, M$. The steps involved in the multistage algorithm correspond to the following.

(1) If N can be written as a product of m pairwise relative primes, for example, $N = a_1 \cdot b_1 \cdot c_1 \ldots$, we can first group N subcarriers into a_1 groups with b_1 subgroups in each group. Then, we index the first-stage groups from 0 to $a_1 - 1$.

(2) Index the second-stage groups in each first-stage group from 0 to $b_1 - 1$. Then group the subcarriers in each second-stage group into c_1 subgroups.

(3) Similar steps continue on until all of the subcarriers are grouped and indexed at the mth-stage.

(4) At the 0th time slot, assign integer set $\{N_k, N_k + M, \ldots, N_k + MN_c\}$ to user k as its FH addresses, where N_k is its access order to the system, $0 < N_k \leq N$.

(5) If $N_k \bmod \{a_1, b_1, c_1, \ldots\} = \{\hat{a}_1, \hat{b}_1, \hat{c}_1, \ldots\}$, then user k first selects the $\hat{b}_1$th second-stage group out of the $\hat{a}_1$th first-stage group, then similar selecting procedures continue on until the subcarrier at the mth-stage has been extracted out for transmission.

(6) The process in step 5 is repeated on the other elements in the integer set of user k until N_c subcarriers have been extracted out for user k to transmit.

(7) At the t_sth time slot, assign integer set $\{N_k + t_s, N_k + M + t_s, \ldots, N_k + MN_c + t_s\}$ as the current FH addresses of user k and repeat steps 5-6.

(8) Repeat steps 4–7 until one mutually orthogonal FH pattern is obtained.

(9) If N can be expressed as products of other combinations of m pairwise relative primes, for example, $N = a_2 \cdot b_2 \cdot c_2 \cdot \cdots = \cdots = a_w \cdot b_w \cdot c_w \ldots$, then w different orthogonal FH patterns can be obtained by repeating steps 1–8, w times.

It is easy to visualize the multistage algorithm by using a tree diagram. An example is given in Figure 3. Here, 30 users access the system ($M = 30$); a total of 30 subcarriers are used, that is, $N = a_1 \cdot b_1 \cdot c_1 = 2 \cdot 3 \cdot 5 = 30$. Two specific examples are illustrated as follows: (1) consider user 2. The subcarriers used by this user at the 0th time slot can be calculated as follows: $2 \bmod \{2, 3, 5\} = \{0, 2, 2\}$; that is, in the 0th first-stage group, the 2nd subcarrier out of the 2nd second-stage group is selected for transmission. This is indicated with a solid line in Figure 3; (2) consider user 27. $27 \bmod \{2, 3, 5\} = \{1, 0, 2\}$; that is, in the 1st first-stage group, the 2nd subcarrier out of the 0th second-stage group is selected by the 27th user for transmission at the 0th time slot. This is indicated with a dashed line in the figure. This procedure continues until an FH sequence of length N is completed. We should note that in this example, the system is fully loaded ($M = N = 30$). For $M < N$, each user

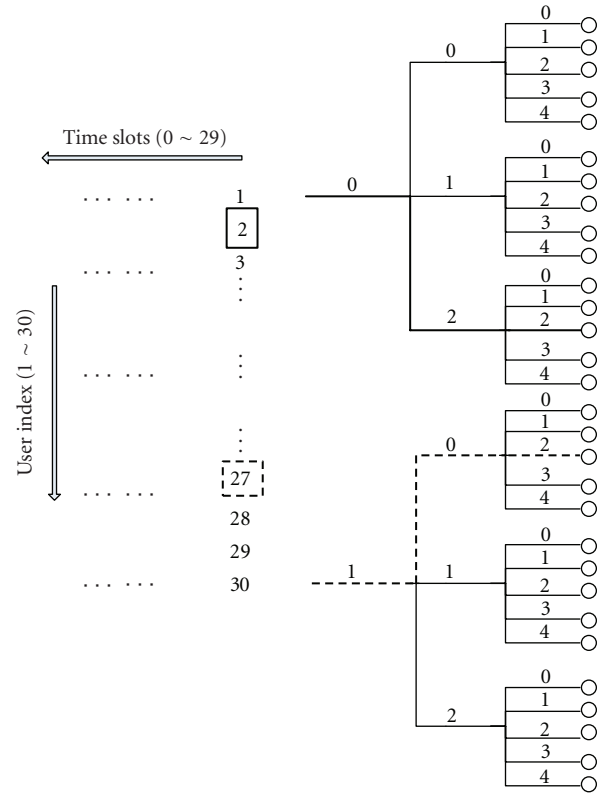

Figure 3: One example of RNS-assisted multistage hopping strategy.

is assigned a set of FH addresses rather than one unique FH signature. For example, consider user 2 in Figure 3, the 2nd subcarrier occupied by user 2 at the 0th time slot is determined starting from his/her current FH address $2+30 = 32$ and following the steps as before. These steps are repeated until N_c subcarriers for user 2 are identified. Extrapolating the procedure across the time axis, an entire FH sequence of length N is designed.

With respect to the design procedures, the major difference between independent hopping and cluster hopping is the following: in independent hopping, each FH address specifies a single subcarrier that can be used. Therefore, if users have very high bandwidth/rate or other QoS requirements, multiple FH addresses can be given to accommodate. In cluster hopping scenario, a user may demand only one unique FH address as a single address completely specifies all N_c subcarriers required for transmission. Fully loaded independent hopping system is a special case of cluster hopping with one subcarrier in each cluster.

From Figures 2 and 3, it is evident that the proposed RNS-FH patterns guarantee the orthogonality among different users within a cell. That is, users within the same cell will not interfere with each other when they simultaneously access the system. The next example, which is shown in Figure 4, demonstrates that if different RNS-FH patterns are assigned to adjacent cells, intercell interferences can be perfectly averaged. In this example, N is set to 10 while the moduli sets used to construct FH patterns in cells 1 and 2 are

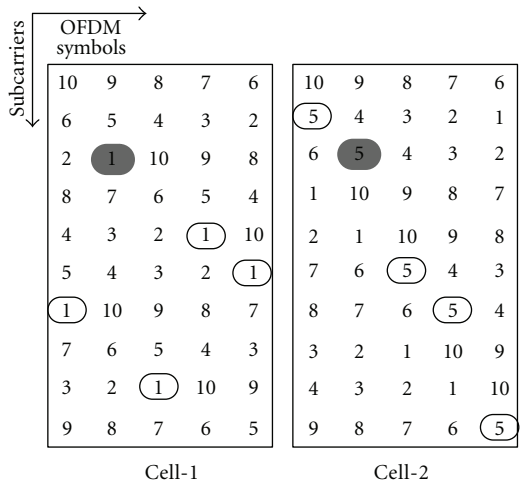

Figure 4: Two different FH patterns are given and their only collision point is highlighted.

$\{a_1 = 2, b_1 = 5\}$ and $\{a_2 = 5, b_2 = 2\}$, respectively. From Figure 4, it is evident that every user in cell 1 experiences interference from different users from cell 2 during each of his/her hops. For example, in the first OFDM symbol duration, user 1 in cell 1 is interfered by user 8 from cell 2; in the next OFDM symbol slot, user 1 is interfered by user 5 from cell 2 and so on. In general, users from different cells collide only once during a frequency hopping cycle under the proposed scheme. Therefore, full interference diversity is exploited in the case of RNS-FH patterns.

The properties of the proposed RNS-FH patterns can be summarized as follows.

(1) At most, a size of $N \times N$ mutually orthogonal FH pattern can be obtained for the independent hopping scheme. The size becomes $M_c \times M_c$ for the cluster hopping.

(2) If N (M_c) can be written as a product of m pairwise relative primes, then at least, $(m-1)m!$ different RNS-FH patterns can be obtained.

(3) With the use of the same moduli set, for independent hopping, RNS-FH patterns constructed after N frames (M_c for cluster hopping) are actually periodical extensions of the RNS-FH pattern designed during the first N (M_c) frames.

(4) With knowledge of moduli and residue, the base station can regenerate the entire RNS-FH pattern using the CRT.

3.3. Comparison with [11]. In this section, we compare our proposed RNS-FH pattern design method with the technique presented in [11] (which also considers RNS as the design metric).

First of all, although both strategies (one proposed here and the other presented in [11]) use the RNS arithmetic as a basis, the mechanisms of determining the hopping sequence are different. In [11], the FH scheme can be visualized as a "top-down" approach where a given bandwidth is divided into multiple candidate subcarriers in multistages according to the predetermined moduli set (see [11, Figure 2]). That is, the choice of the moduli set (top level decision) determines the number of subcarriers that can be used (bottom level decision) for hopping. This scheme is driven in conjunction with MFSK-modulated signals and a reference register **C**, which has the same length as the moduli set (v), providing reference to each user in order to enable synchronous transmission. However, in our work, we assume that the division of the frequency bandwidth has already been done in advance. That is, the number of subcarriers that can be used for hopping is given (bottom level decision). Based on this number, we employ a proper moduli set to group and index each of the candidate subcarriers (top level decision). Therefore, we can interpret our proposed initialization process as a "bottom-up" approach (see Figure 3). It is important to note that in practical OFDMA cellular systems, the division of the bandwidth within a cell is usually fixed and predetermined (e.g., 1024 subcarriers). Therefore, our "bottom-up" approach is more suitable for such practical systems. Furthermore, unlike the length-v reference register **C** that is used in [11], the FH scheme proposed in this paper invokes the use of only a length-one register to store the time index which in turn can be used to calculate current FH address of each user at the base station.

Secondly, for reducing intercell interference, [11] suggests the use of different moduli sets for adjacent cells. Since the choice of the moduli set determines the number of subcarriers used for hopping, a different moduli set in adjacent cells will result in different number of subcarriers in adjacent cells. If the total bandwidth is the same for all cells, this approach translates into subcarriers in adjacent cells having different bandwidths. This may be an unrealistic assumption for practical OFDMA systems. If the method in [11] is applied to a practical scenario using fixed number of subcarriers (each with the same bandwidth), high intercell interference will result (as shown in Figure 8). Our proposed "bottom-up" approach does not suffer from this drawback as it is built on the premise that the number of subcarriers and their bandwidths are fixed across cells.

In summary, the method proposed in this work is flexible and well suited for practical OFDMA cellular systems.

4. Simulation Results

Parameters of the simulated system are provided in Table 1. The cyclic prefix within one OFDM symbol duration is assumed long enough to eliminate ISI (intersymbol interference). Two 6-ray channel pulse responses are considered following the UTRA vehicular test environment [16]. In Figure 5, the correlation functions of these two channels are plotted versus the variation of Δf, while $\Delta t = 1$ slot and $f_D T_s = 0.01$. From Figure 5, we can conclude that if small hopping intervals occur frequently in an FH pattern, Veh B can provide more frequency diversity than Veh A.

Theoretical (see (10) and (12)) and simulated expected number of collisions per symbol in RNS-FH OFDMA are

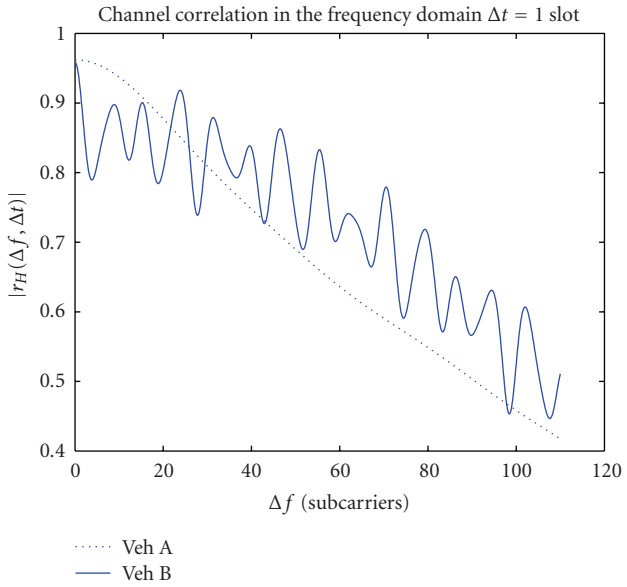

Figure 5: Channel correlation function.

Table 1: System parameters.

Transmission BW	5 MHz
Carrier frequency	2 GHz
OFDM symbol duration	100 μs
CP duration	10 μs
Tone spacing	11 KHz
FFT size	128
Occupied subcarriers	110
Channel impulse response	Veh A/Veh B
Channel coding	1/2 convolutional code
Modulation	QPSK
Time slots	10

given in Figure 6. The high collision probability severely limits the number of active users that can be simultaneously supported by the FH system.

In Figure 7, bit error rate (BER) versus SNR of RNS-FH OFDMA under both cluster and independent hopping is plotted. The main objective of this example is to characterize the effects of frequency diversity exploited by RNS-FH patterns on system performance. Here, we assume that 10 users are in the system with 11 subcarriers assigned to each via the two-stage RNS hopping strategy. For cluster hopping, the moduli set used is $\{a_1 = 2, b_1 = 5\}$, while for independent hopping, it is $\{a_1 = 2, b_1 = 55\}$. It is observed that both independent and clustered RNS-FH OFDMA dramaticallyoutperforms the regular OFDMA scheme without hopping in both Veh A and Veh B environments. Another observation is that under both independent and cluster hopping, the system performs better in Veh A. That is, in the proposed RNS-FH patterns, large hopping intervals occur more frequently than small hopping distances. This characteristic is very important since it reveals that users occupy a wide bandwidth during a small fraction of all hops.

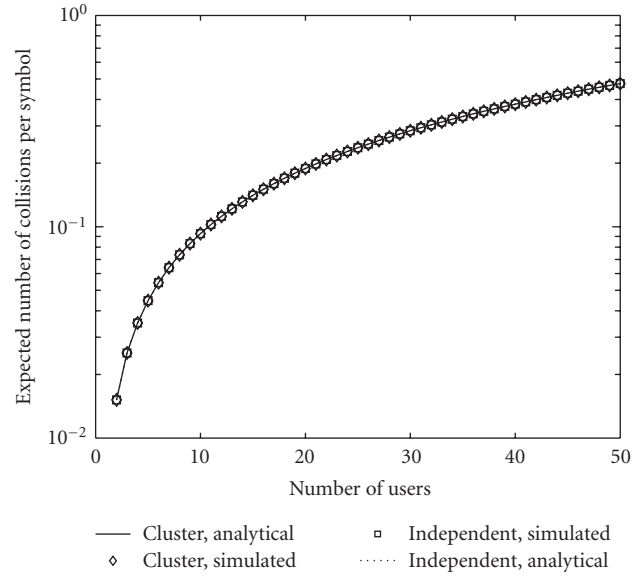

Figure 6: Expected number of collisions per symbol versus the number of users.

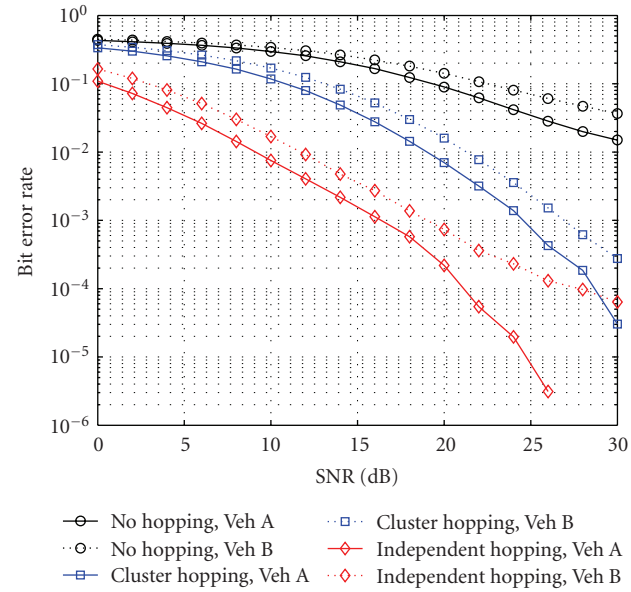

Figure 7: BER versus SNR of RNS-FH OFDMA under cluster and independent hopping with different channel conditions. $N = 110$, $M = M_c = 10$, $N_c = 11$, $f_D T_s = 0.01$.

Furthermore, since independent hopping scheme results in a much larger FH pattern than cluster hopping, more frequency diversity can be exploited in the independent hopping case. This is also clearly reflected by the simulation results shown in Figure 7. For example, at a BER level of 10^{-3}, nearly 8 dB gain is offered by independent hopping relative to cluster hopping in Veh A environment.

Figure 8 quantifies the intercell interferences experienced by different users in the cell of interest, averaged across time. The x-axis represents the indices of the users within

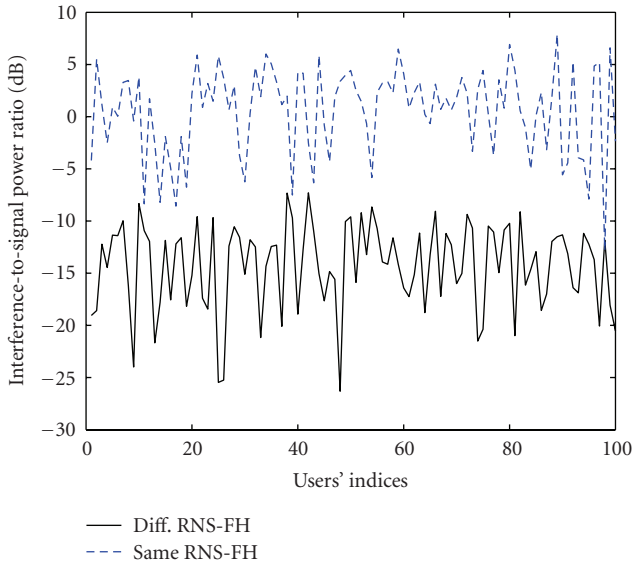

FIGURE 8: Intercell interference-to-signal power ratio for given users under different RNS-FH patterns and identical RNS-FH patterns assignments across cells.

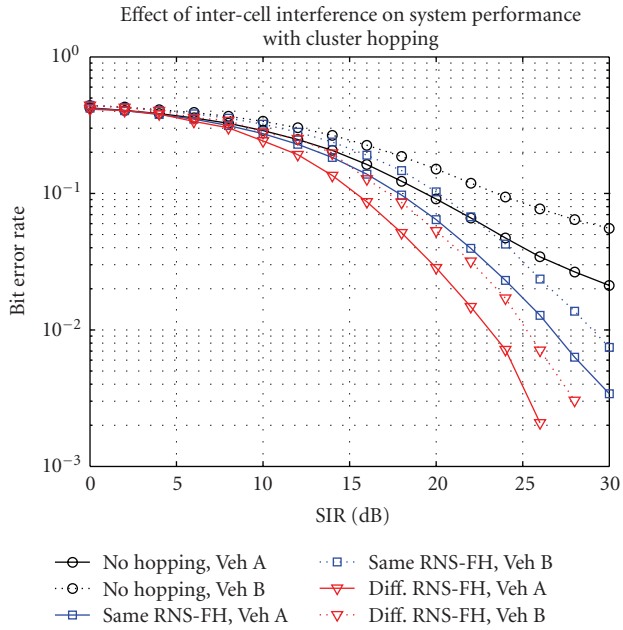

FIGURE 9: BER versus SIR of RNS-FH OFDMA under cluster hopping with different channel conditions. $N = 110$, $M = M_c = 10$, $N_c = 11$, SNR = 25 dB, $f_D T_s = 0.01$.

the cell of interest while the y-axis characterizes the time-averaged intercell interference-to-signal power ratio for a given user. Two situations are considered: (1) different RNS-FH patterns are allocated to the cell of interest and the interfering cell (denoted by the solid line); (2) the same RNS-FH pattern as the cell of interest is assigned to the interfering cell (denoted by the dashed line). Here, we model the intercell interference as additive Gaussian-distributed distortion. Therefore, in scenario (1), users in the cell of interest will experience different interferences from the interfering cell across all hops, which in turn induces interference diversity. Figure 8 clearly demonstrates that by employing the proposed method (i.e., allocating a different RNS-FH pattern to the interfering cell), the intercell interference floor can be significantly lowered relative to the scenario where all cells employ identical RNS-FH patterns.

Figures 9 and 10 show the effects of intercell interference diversity on system performance. BER versus signal-to-interference ratio (SIR) is plotted under cluster and independent hopping in Figures 9 and 10, respectively. For cluster hopping, the FH pattern assigned to the interfering cell is constructed by using $\{a_2 = 5, b_2 = 2\}$ while it is $\{a_2 = 55, b_2 = 2\}$ for the independent hopping scenario. We simulate the case where the same RNS-FH pattern used in the cell of interest is assigned to adjacent interfering cells. Thus, users in the cell of interest will be affected by the same interferences from adjacent cells during all hops. Therefore, no interference diversity is exploited. Simulation results also reflect this feature. When the same RNS-FH pattern is assigned, frequency diversity as a result of hopping reduces the interference floor. Therefore, the no hopping case still exhibits the worst BER performance. When different patterns are allocated to interfering cells, the interference diversity along with frequency diversity further improves

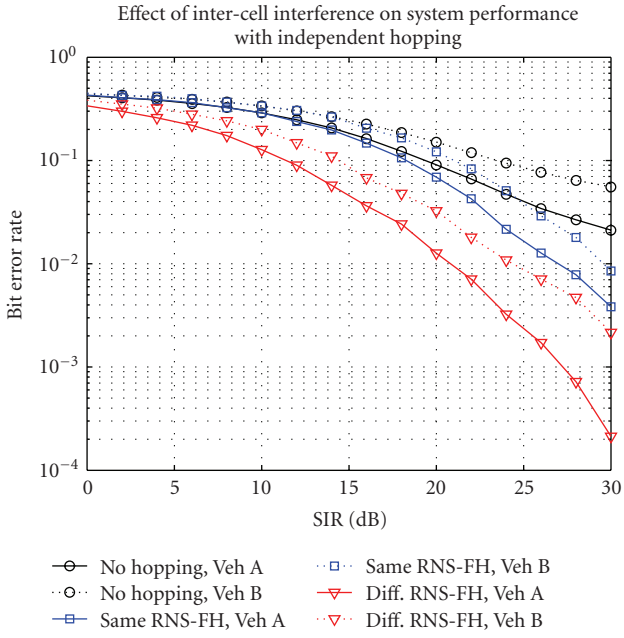

FIGURE 10: BER versus SIR of RNS-FH OFDMA under independent hopping with different channel conditions. $N = 110$, $M = M_c = 10$, $N_c = 11$, SNR = 25 dB, $f_D T_s = 0.01$.

system BER performance. For example, in cluster hopping (Figure 9), with different pattern assignments, nearly 3 dB gain at a BER level of 10^{-2} is achieved relative to the system employing identical hopping. This gain grows to 5 dB under independent hopping scenario (Veh B environment).

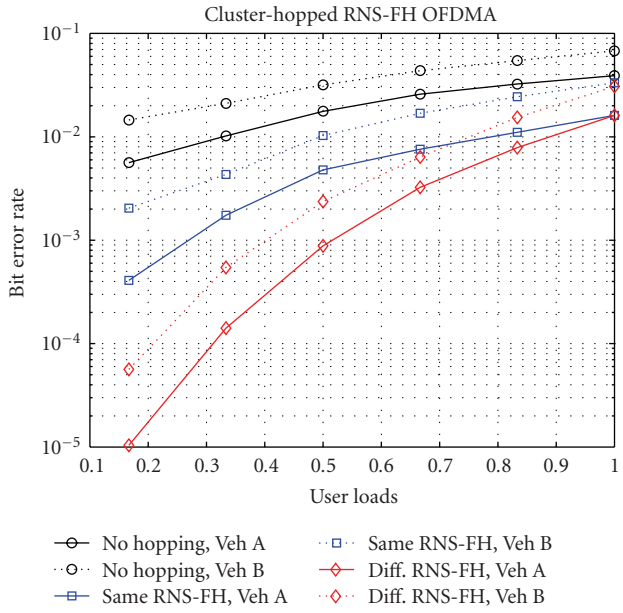

Figure 11: BER versus user loads of RNS-FH OFDMA under cluster hopping with different channel conditions, $N = 110$, $M = M_c = 10$, $N_c = 11$, SNR = 25 dB, SIR = 15 dB, $f_D T_s = 0.01$.

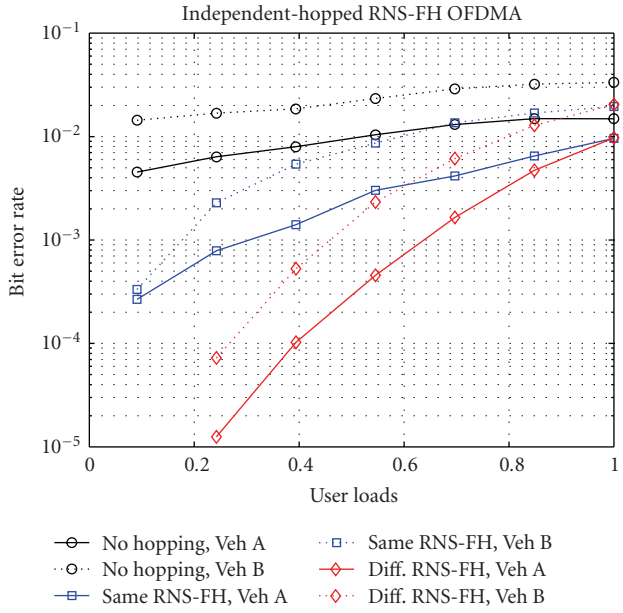

Figure 12: BER versus user loads of RNS-FH OFDMA under independent hopping with different channel conditions, $N = 110$, $M = M_c = 10$, $N_c = 11$, SNR = 25 dB, SIR = 15 dB, $f_D T_s = 0.01$.

BER versus user loads is plotted in Figures 11 and 12 under cluster and independent hopping, respectively, in both Veh A and Veh B. Effects of frequency and interference diversities on system performance are explored at given SNR and SIR. It is evident that the system throughput can be significantly enhanced by assigning different RNS-FH patterns to different cells, while it is severely limited

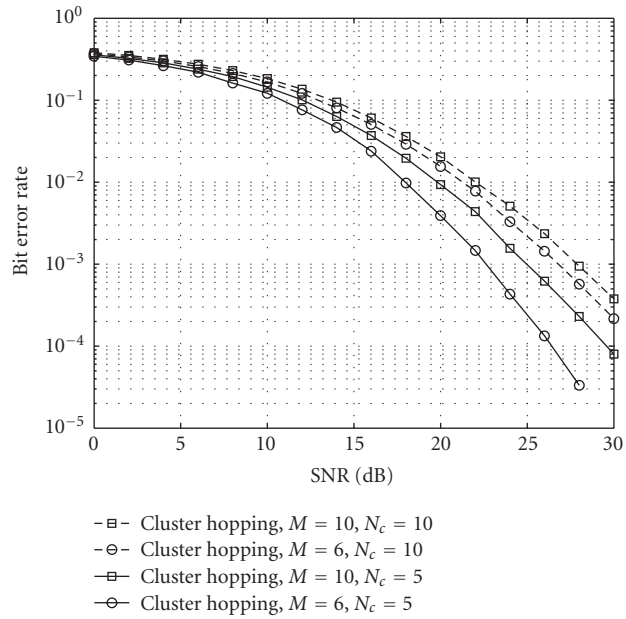

Figure 13: Performance of cluster-hopped RNS-FH OFDMA with different cluster sizes and different number of active users, $f_D T_s = 0.01$.

if no hopping occurs. Furthermore, the performance gap between the identical hopping and the different hopping decreases with the increase in user loads. That is, the benefit of intercell interference diversity is greater for lower user loads.

Figure 13 illustrates that by increasing the cluster size (the number of subcarriers in one cluster), or the number of active users, the number of collisions increases. This in turn induces degradation in BER performance as can be seen from Figure 13.

Finally, we compare our proposed RNS-FH pattern design strategy with state-of-the-art FH pattern designs. Specifically, our benchmark for comparison is the Latin squares (LSs-)-aided FH pattern design presented in [6]. In our proposed RNS-FH pattern, the spacing between hops in time and frequency is far enough that subcarriers employed in a single time slot are weakly correlated. This feature provides remarkable performance improvements that are consistent across all cells. However, in Latin squares (LSs-)-aided FH pattern design, performances in different cells may vary a lot. Relative comparisons are given in Figure 14, where two Latin squares-based FH patterns A_4 and A_{38} [6] are employed. In LS A_{38}, smaller hops happen more frequently, and for such smaller hops, Veh B exploits more frequency diversity than Veh A. The opposite is also true for LS A_4. Using simulation results, we first observe that in RNS-aided FH-OFDMA, different RNS-FH patterns provide nearly the same BER performance, while it varies a lot in LS-aided FH-OFDMA; the second observation is that our proposed RNS-FH patterns have similar BER performances to LS A_4 while outperforming LS A_{38}. Although there may exist LS-aided FH pattern that has better performance than the proposed

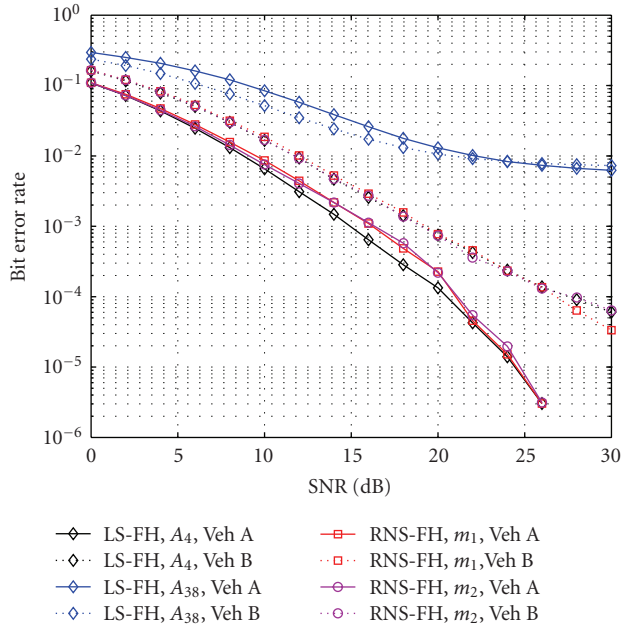

FIGURE 14: Performance of independent-hopped RNS-FH OFDMA versus LS-FH OFDMA, $N = 110$, $M = M_c = 10$, $N_c = 11$, LS A_4 and A_{38} are used, different moduli sets $m_1 = \{2, 55\}$ and $m_2 = \{2, 11, 5\}$ are applied to construct RNS-FH patterns, $f_D T_s = 0.01$.

scheme, the performance variations in LS-aided FH pattern design really limit their applications.

5. Conclusions

In this paper, we propose an RNS arithmetic-based FH pattern design that is well suited and easy to implement for practical OFDMA cellular systems. RNS-FH patterns not only guarantee zero collision within a cell, but also average the intercell interferences by assigning different FH patterns to adjacent cells. Additionally, by having a large spacing between the hopping frequencies, the RNS-FH patterns exploit frequency diversity effectively and provide significant improvement in BER performance. The BER performance gain is consistent across all cells unlike other FH pattern design schemes such as the LS-based method where wide performance variations are observed across cells. Simulation experiments demonstrate the superior performance of the RNS-FH scheme in terms of frequency diversity and intercell interference diversity under both independent and cluster hopping strategies.

References

[1] S. Gault, W. Hachem, and P. Ciblat, "Performance analysis of an OFDMA transmission system in a multicell environment," *IEEE Transactions on Communications*, vol. 55, no. 4, pp. 740–751, 2007.

[2] M. K. Simon, J. K. Omura, R. A. Scoltz, and B. K. Levitt, *Spread Spectrum Communications*, Computer Science Press, Rockville, Md, USA, 1985.

[3] T. Scholand, T. Faber, A. Seebens, et al., "Fast frequency hopping OFDM concept," *Electronics Letters*, vol. 41, no. 13, pp. 748–749, 2005.

[4] T. Kurt and H. Deliç, "On symbol collisions in FH-OFDMA," in *Proceedings of the 59th IEEE Vehicular Technology Conference (VTC '04)*, vol. 4, pp. 1859–1863, Milan, Italy, May 2004.

[5] T. Kurt and H. Deliç, "Space-frequency coding reduces the collision rate in FH-OFDMA," *IEEE Transactions on Wireless Communications*, vol. 4, no. 5, pp. 2045–2049, 2005.

[6] K. Stamatiou and J. G. Proakis, "A performance analysis of coded frequency-hopped OFDMA," in *Proceedings of IEEE Wireless Communications and Networking Conference (WCNC '05)*, vol. 2, pp. 1132–1137, New Orleans, La, USA, March 2005.

[7] S. V. Maric and O. Moreno, "Using costas arrays to construct frequency hop patterns for OFDM wireless systems," in *Proceedings of the 40th IEEE Conference on Information Sciences and Systems (CISS '06)*, pp. 505–507, Princeton, NJ, USA, March 2007.

[8] C. Wang, X. Zhang, and D. Yang, "Evaluation of welch-costas frequency hopping pattern for OFDM cellular system," in *Proceedings of the 18th IEEE International Symposium on Personal, Indoor and Mobile Radio Communications (PIMRC '07)*, pp. 1–5, Athens, Greece, September 2007.

[9] T. Li, Q. Ling, and J. Ren, "A spectrally efficient frequency hopping system," in *Proceedings of the 50th IEEE Global Telecommunications Conference (GLOBECOM '07)*, pp. 2997–3001, Washington, DC, USA, November 2007.

[10] B. M. Popovic and Y. Li, "Frequency-hopping pilot patterns for OFDM cellular systems," *IEICE Transactions on Fundamentals of Electronics, Communications and Computer Sciences*, vol. E89-A, no. 9, pp. 2322–2328, 2006.

[11] L.-L. Yang and L. Hanzo, "Residue number system assisted fast frequency-hopped synchronous ultra-wideband spread-spectrum multiple-access: a design alternative to impulse radio," *IEEE Journal on Selected Areas in Communications*, vol. 20, no. 9, pp. 1652–1663, 2002.

[12] J. Chen, T. Lv, and H. Zheng, "Joint cross-layer design for wireless QoS content delivery," in *Proceedings of IEEE International Conference on Communications (ICC '04)*, vol. 7, pp. 4243–4247, Paris, France, June 2004.

[13] J. G. Proakis, *Digital Communications*, McGraw Hill, New York, NY, USA, 4th edition, 2001.

[14] K. W. Watson and C. W. Hastings, "Self-checked computation using residue arithmetic," *Poceeding of the IEEE*, vol. 54, no. 12, pp. 1920–1931, 1966.

[15] L.-L. Yang and L. Hanzo, "Redundant residue number system based error correction codes," in *Proceedings of the 54th IEEE Vehicular Technology Conference (VTC '01)*, vol. 3, pp. 1472–1476, Atlantic City, NJ, USA, October 2001.

[16] *ETSI TR 101 112, UMTS 30.03, V3.1.0, Annex B, Std.*